

Fermionic decay of charged Higgs boson in low mass region in Georgi Machacek Model

Swagata Ghosh^{a,b,*}

^a *Department of Physics and Astrophysics, University of Delhi, Delhi, India.*

^b *SGTB Khalsa College, University of Delhi, Delhi, India.*

Abstract

At the Large Hadron Collider (LHC), ATLAS and CMS collaborations observed various decay modes of the light charged Higgs bosons produced by top (anti)quark decays. In this paper, we are interested in the subsequent decay of the light charged Higgs boson into a charm and a strange quark-antiquark pair and into a tau and a tau-neutrino pair, separately, in the context of the Georgi-Machacek model, which offers a large triplet vacuum expectation value (vev) preserving custodial symmetry. We show that these experimental observations constrain the triplet vev from above. We explore the model parameter space consistent with the theoretical constraints, the latest Higgs data and the experimental data for light charged Higgs decaying to cs and $\tau\nu_\tau$.

1 Introduction

The discovery of the Higgs boson with a mass around 125 GeV at the Large Hadron Collider (LHC) experiment [1, 2] in the year of 2012 let the Standard Model (SM) have great success. The possibility of having new exotic particles still cannot be thrown away. It is always possible that the discovered 125 GeV scalar resonance is a part of a non-minimal Higgs sector accommodating one or more non-standard scalar multiplets. Besides, the new beyond Standard Model (BSM) scalar can be neutral or charged.

With an appealing phenomenology, the physical charged scalars got searched at LHC prolongedly. These charged scalars can be lighter as well as heavier than the top quark mass (m_t). At LHC, light charged scalar decaying to cb [3, 4], cs [5–7], and $\tau\nu_\tau$ [9–15] is searched. Besides, light charged scalars decay in different multi-Higgs doublet models [16–21] and in other colliders [22–24] are also searched and studied.

Most of the BSM models with extended scalar sectors commit singly charged scalar particle, through which one can explore the model parameter space. In this paper, we consider the Georgi-Machacek (GM) Model [25], where both of the singly and doubly charged scalars are present, though we focus only on the decay of the singly charged scalar when its mass is in the range of 80-160 GeV.

The GM model is atypical of the other triplet extensions of the SM as it preserves the custodial symmetry in the tree level, i.e., the ρ -parameter is equal to unity in this model, hence resulting in a sizeable triplet vacuum expectation value (VEV), v_2 . In the GM model, the extended scalar sector contains one real triplet and one complex triplet, neutral components of both possessing the same VEV. The physical scalar sector includes ten scalars ordered as two singlets, one triplet, and one quintuplet. Out of these ten scalars, 4 scalars are charge-neutral (h , H , H_3^0 , H_5^0), another 4 are singly-charged (H_3^\pm , H_5^\pm), and the rest 2 scalars are doubly-charged ($H_5^{\pm\pm}$). The two singly-charged scalars H_5^\pm do not couple to the SM fermions, whereas, the other two singly-charged scalars H_3^\pm couple to the SM fermions, and the strength of coupling is directly proportional to the triplet VEV v_2 , which is sizeable enough in the GM model. We will focus on the decay of the H_3^\pm in this paper.

Decay of charged scalar, heavier than the top quark mass, is studied in the context of the Georgi-Machacek model [26, 27]. The theoretical limits [28–32] on the Lagrangian parameters, the indirect constraints [33], Higgs boson pair productions at the LHC [34], electroweak phase transition [35, 36], impacts of higher dimensional operators [37] in the Georgi-Machacek model are well scrutinized. For phenomenological studies of this model at the LHC [38], electron-positron collider [39], the reader may

*swgtghsh54@gmail.com

also consult the literature. There are also some variants of the GM model [40, 41]. One can scan the parameter space of this model using the calculator [42]. For the global fits in the GM model, see [43]. It is to be mentioned here that, inspite of the extensive phenomenological study of the GM model, the exploration of the parameter space in case of the light charged scalar together with the LHC data has not been examined as yet.

This paper is organized as follows. In Sec. 2 we describe the model in brief. We enlist the theoretical constraints and LHC data, with their effects on the parameter space of the GM model in Sec. 3. The results are given in Sec. 4. Finally we conclude in Sec. 5.

2 The Georgi-Machacek Model

One $SU(2)_L$ real triplet $(\xi^+, \xi^0, \xi^-)^T$ with hypercharge $Y = 0$ and one $SU(2)_L$ complex triplet $(\chi^{++}, \chi^+, \chi^0)^T$ with $Y = 2$ are appended to the particle contents of the scalar sector of the Standard Model to obtain the Georgi-Machacek model. We mostly persue the notations followed in [29] throughout this paper.

The SM doublet $(\phi^+, \phi^0)^T$ with $Y = 1$ and the non-standard triplets can be expressed in terms of bi-doublet and bi-triplet respectively, as,

$$\Phi = \begin{pmatrix} \phi^{0*} & \phi^+ \\ \phi^- & \phi^0 \end{pmatrix}, \quad X = \begin{pmatrix} \chi^{0*} & \xi^+ & \chi^{++} \\ \chi^- & \xi^0 & \chi^+ \\ \chi^{--} & \xi^- & \chi^0 \end{pmatrix}. \quad (1)$$

The most general scalar potential is given by,

$$\begin{aligned} V(\Phi, X) = & \frac{\mu_2^2}{2} \text{Tr}(\Phi^\dagger \Phi) + \frac{\mu_3^2}{2} \text{Tr}(X^\dagger X) + \lambda_1 [\text{Tr}(\Phi^\dagger \Phi)]^2 + \lambda_2 \text{Tr}(\Phi^\dagger \Phi) \text{Tr}(X^\dagger X) \\ & + \lambda_3 \text{Tr}(X^\dagger X X^\dagger X) + \lambda_4 [\text{Tr}(X^\dagger X)]^2 - \lambda_5 \text{Tr}(\Phi^\dagger \tau^a \Phi \tau^b) \text{Tr}(X^\dagger t^a X t^b) \\ & - M_1 \text{Tr}(\Phi^\dagger \tau^a \Phi \tau^b) (UXU^\dagger)_{ab} - M_2 \text{Tr}(X^\dagger t^a X t^b) (UXU^\dagger)_{ab}, \end{aligned} \quad (2)$$

with $\tau^a = \sigma^a/2$, where σ^a are the three Pauli matrices, and the t^a s as,

$$t^1 = \frac{1}{\sqrt{2}} \begin{pmatrix} 0 & 1 & 0 \\ 1 & 0 & 1 \\ 0 & 1 & 0 \end{pmatrix}, t^2 = \frac{1}{\sqrt{2}} \begin{pmatrix} 0 & -i & 0 \\ i & 0 & -i \\ 0 & i & 0 \end{pmatrix}, t^3 = \begin{pmatrix} 1 & 0 & 0 \\ 0 & 0 & 0 \\ 0 & 0 & -1 \end{pmatrix}. \quad (3)$$

The matrix U in the trilinear terms of the GM potential is given by,

$$U = \frac{1}{\sqrt{2}} \begin{pmatrix} -1 & 0 & 1 \\ -i & 0 & -i \\ 0 & \sqrt{2} & 0 \end{pmatrix}. \quad (4)$$

After the electroweak symmetry breaking (EWSB), the neutral components of the bi-doublet and the bi-triplet acquire the VEVs, as,

$$\langle \phi^0 \rangle = \frac{v_1}{\sqrt{2}}, \quad \langle \chi^0 \rangle = \langle \xi^0 \rangle = v_2. \quad (5)$$

Note that, the equality of the real and complex triplet VEVs corresponds to the preservation of the custodial symmetry of the potential at the tree level leading to $\rho_{\text{tree}} = 1$.

The EW VEV v relates to the doublet and triplet VEVs as,

$$\sqrt{v_1^2 + 8v_2^2} = v \approx 246 \text{ GeV}. \quad (6)$$

The doublet-triplet mixing angle may be expressed as,

$$\tan \beta = \frac{2\sqrt{2}v_2}{v_1}, \quad (7)$$

In terms of VEVs given in Eq. (5), the potential (2) becomes

$$\begin{aligned} V(v_1, v_2) = & \frac{\mu_2^2}{2}v_1^2 + 3\frac{\mu_3^2}{2}v_2^2 + \lambda_1 v_1^4 + \frac{3}{2}(2\lambda_2 - \lambda_5)v_1^2 v_2^2 \\ & + 3(\lambda_3 + 3\lambda_4)v_2^4 - \frac{3}{4}M_1 v_1^2 v_2 - 6M_2 v_2^3, \end{aligned} \quad (8)$$

Hence, using the extremisation conditions one can easily extract the bilinear coefficients of the potential as,

$$\begin{aligned} \mu_2^2 = & -4\lambda_1 v_1^2 - 3(2\lambda_2 - \lambda_5)v_2^2 + \frac{3}{2}M_1 v_2, \\ \mu_3^2 = & -(2\lambda_2 - \lambda_5)v_1^2 - 4(\lambda_3 + 3\lambda_4)v_2^2 + \frac{M_1 v_1^2}{4v_2} + 6M_2 v_2. \end{aligned} \quad (9)$$

The scalar sector of the GM model consists of ten physical fields of which five are part of a custodial quintuplet $H_5 = (H_5^{++}, H_5^+, H_5^0, H_5^-, H_5^{--})^T$, three are part of a custodial triplet $H_3 = (H_3^+, H_3^0, H_3^-)^T$, and the rest two are custodial singlets H_1^0 and $H_1^{0'}$. These ten physical fields may be expressed in terms of the component fields and the angle β as,

$$\begin{aligned} H_5^{++} = \chi^{++}, \quad H_5^+ = \frac{(\chi^+ - \xi^+)}{\sqrt{2}}, \quad H_5^0 = \sqrt{\frac{2}{3}}\xi^0 - \sqrt{\frac{1}{3}}\chi^{0R}, \\ H_3^+ = -\sin\beta\phi^+ + \cos\beta\frac{(\chi^+ + \xi^+)}{\sqrt{2}}, \quad H_3^0 = -\sin\beta\phi^{0I} + \cos\beta\chi^{0I}, \\ H_1^0 = \phi^{0R}, \quad H_1^{0'} = \sqrt{\frac{1}{3}}\xi^0 + \sqrt{\frac{2}{3}}\chi^{0R}. \end{aligned} \quad (10)$$

The physical fields of the multiplets are mass degenerate. The square of the common mass of the quintuplet H_5 and the triplet H_3 are given by,

$$\begin{aligned} m_5^2 = & \frac{M_1}{4v_2}v_1^2 + 12M_2 v_2 + \frac{3}{2}\lambda_5 v_1^2 + 8\lambda_3 v_2^2, \\ m_3^2 = & \left(\frac{M_1}{4v_2} + \frac{\lambda_5}{2}\right)v^2, \end{aligned} \quad (11)$$

respectively.

The custodial singlets H_1^0 and $H_1^{0'}$ mix to yield the mass eigenstates h and H as,

$$\begin{aligned} h &= \cos\alpha H_1^0 - \sin\alpha H_1^{0'}, \\ H &= \sin\alpha H_1^0 + \cos\alpha H_1^{0'}, \end{aligned} \quad (12)$$

with the mass squared matrix

$$\mathcal{M}^2 = \begin{pmatrix} \mathcal{M}_{11}^2 & \mathcal{M}_{12}^2 \\ \mathcal{M}_{21}^2 & \mathcal{M}_{22}^2 \end{pmatrix}, \quad (13)$$

where

$$\begin{aligned} \mathcal{M}_{11}^2 &= 8\lambda_1 v_1^2, \\ \mathcal{M}_{12}^2 &= \mathcal{M}_{21}^2 = \frac{\sqrt{3}}{2}[-M_1 + 4(2\lambda_2 - \lambda_5)v_2]v_1, \\ \mathcal{M}_{22}^2 &= \frac{M_1 v_1^2}{4v_2}. \end{aligned} \quad (14)$$

The neutral scalar mixing angle α can be parametrised in terms of the components of the mass-squared matrix as,

$$\tan 2\alpha = \frac{2\mathcal{M}_{12}^2}{\mathcal{M}_{22}^2 - \mathcal{M}_{11}^2}. \quad (15)$$

The mass-squared of the physical neutral scalars are,

$$m_{h,H}^2 = \frac{1}{2} \left[\mathcal{M}_{11}^2 + \mathcal{M}_{22}^2 \mp \sqrt{(\mathcal{M}_{11}^2 - \mathcal{M}_{22}^2)^2 + 4(\mathcal{M}_{12}^2)^2} \right]. \quad (16)$$

We assume here that $m_H > m_h$ and consider the CP-even neutral scalar with smaller mass as the SM-like Higgs boson, such that $m_h \approx 125$ GeV.

The bilinear couplings (μ_2^2 and μ_3^2) present in the scalar potential are already traded in terms of the VEVs v_1 and v_2 in the Eq. (9). The quartic couplings λ_i ($i = 1$ to 5) in the potential (2) can be expressed in terms of the four physical masses, m_h , m_H , m_3 , m_5 , and the mixing angle α as,

$$\begin{aligned} \lambda_1 &= \frac{1}{8v_1^2} (m_h^2 \cos^2 \alpha + m_H^2 \sin^2 \alpha), \\ \lambda_2 &= \frac{1}{8v_2} \left[- (m_H^2 - m_h^2) \frac{1}{\sqrt{3}v_1} \sin 2\alpha - M_1 + 8m_3^2 \frac{v_2}{v^2} \right], \\ \lambda_3 &= \frac{1}{8v_2^2} \left(m_5^2 - 3m_3^2 \frac{v_1^2}{v^2} + \frac{M_1 v_1^2}{2v_2} - 12M_2 v_2 \right), \\ \lambda_4 &= \frac{1}{24v_2^2} \left(m_h^2 \sin^2 \alpha + m_H^2 \cos^2 \alpha - m_5^2 + 3m_3^2 \frac{v_1^2}{v^2} - 3M_1 \frac{v_1^2}{4v_2} + 18M_2 v_2 \right), \\ \lambda_5 &= 2 \left(\frac{m_3^2}{v^2} - \frac{M_1}{4v_2} \right). \end{aligned} \quad (17)$$

3 Theoretical constraints and LHC data

The theoretical constraints, mainly resulting from the perturbative unitarity and electroweak vacuum stability, and the experimental constraints, typically following the LHC data put the limit on the parameters of the GM potential. Here, we write down the theoretical constraints already available in the literature. The reader may follow [29, 33] for the detailed knowledges of the theoretical constraints.

Constraints obtained from perturbative unitarity are given by,

$$\begin{aligned} \sqrt{(6\lambda_1 - 7\lambda_3 - 11\lambda_4)^2 + 36\lambda_2^2} + |6\lambda_1 + 7\lambda_3 + 11\lambda_4| &< 4\pi, \\ \sqrt{(2\lambda_1 + \lambda_3 - 2\lambda_4)^2 + \lambda_5^2} + |2\lambda_1 - \lambda_3 + 2\lambda_4| &< 4\pi, \\ |2\lambda_3 + \lambda_4| &< \pi, \\ |\lambda_2 - \lambda_5| &< 2\pi, \end{aligned} \quad (18)$$

and the constraints obtained from electroweak vacuum stability are given by,

$$\begin{aligned} \lambda_1 &> 0, \\ \lambda_2 + \lambda_3 &> 0, \\ \lambda_2 + \frac{1}{2}\lambda_3 &> 0, \\ -|\lambda_4| + 2\sqrt{\lambda_1(\lambda_2 + \lambda_3)} &> 0, \\ \lambda_4 - \frac{1}{4}|\lambda_5| + \sqrt{2\lambda_1(2\lambda_2 + \lambda_3)} &> 0. \end{aligned} \quad (19)$$

For the constraints coming from the LHC data, we consider the Higgs data at $\sqrt{s}=13$ TeV [44, 45]. Here, we contemplate the lightest CP-even scalar h as the SM-like Higgs with mass $m_h \approx 125$ GeV. Therefore, we require to know the couplings of h with the SM fermions and the vector bosons, which we enlist below :

$$g_{h\bar{f}f} = -i \frac{m_f}{v} \frac{c_\alpha}{c_\beta}, \quad ig_{hWW}\eta_{\mu\nu} = ic_W^2 g_{hZZ}\eta_{\mu\nu} = -i \frac{e^2}{6s_W^2} (8\sqrt{3}s_\alpha v_2 - 3c_\alpha v_1)\eta_{\mu\nu}. \quad (20)$$

The ratio of the fermionic and bosonic couplings with h in the GM model to that in the SM model are given by,

$$\kappa_f^h = \frac{v}{v_1} c_\alpha, \quad \kappa_V^h = -\frac{1}{3v} (8\sqrt{3}s_\alpha v_2 - 3c_\alpha v_1). \quad (21)$$

For the decay $h \rightarrow \gamma\gamma$, the charged scalars coming from the triplet and quintuplet contribute in the loop. So, we need the corresponding couplings :

$$\begin{aligned} -ig_{hH_3^+H_3^-} &= -i(64\lambda_1 c_\alpha \frac{v_2^2 v_1}{v^2} - \frac{8}{\sqrt{3}} \frac{v_1^2 v_2}{v^2} s_\alpha (\lambda_3 + 3\lambda_4) - \frac{4}{\sqrt{3}} \frac{v_2 M_1}{v^2} (s_\alpha v_2 - \sqrt{3} c_\alpha v_1) \\ &\quad - \frac{16}{\sqrt{3}} \frac{v_2^3}{v^2} s_\alpha (6\lambda_2 + \lambda_5) - c_\alpha \frac{v_1^3}{v^2} (\lambda_5 - 4\lambda_2) + 2\sqrt{3} M_2 \frac{v_1^2}{v^2} s_\alpha \\ &\quad - \frac{8}{\sqrt{3}} \lambda_5 \frac{v_1 v_2}{v^2} (s_\alpha v_1 - \sqrt{3} c_\alpha v_2)), \\ -ig_{hH_5^+H_5^-} &= -ig_{hH_5^{++}H_5^{--}} = -i(-8\sqrt{3}(\lambda_3 + \lambda_4)s_\alpha v_2 + (4\lambda_2 + \lambda_5)c_\alpha v_1 - 2\sqrt{3}M_2 s_\alpha). \end{aligned} \quad (22)$$

One can replace the λ_i s present in the Eq. (22) with the help of the expressions given in (17) to get the couplings in terms of the physical masses, mixing angle, VEVs, and the trilinear coefficients.

Considering the Eq. (9) and (17), we have nine independent parameters ($m_h, m_H, m_3, m_5, \sin \alpha, v_2, v, M_1, M_2$) and we choose m_h as identical to the SM-like Higgs mass. To scan the parameter space, we choose the mass of the heavier CP-even neutral scalar H starting from 150 GeV and that of the members of the multiplets starting from 80 GeV. The upper limit of m_H and m_5 are set to 1000 GeV. We vary the triplet VEV v_2 in between 0 – 60 GeV. v is the electroweak VEV as usual. Since our purpose is to study the low mass phenomenology of H_3^+ , we consider m_3 in between 80 – 160 GeV. Finally, we consider M_1 and M_2 in between $[-2000, 2000]$ GeV.

Now, in Fig. (1) we present the plots in the $m_3 - v_2, m_5 - v_2, m_3 - m_5, m_H - v_2, v_2 - M_1, v_2 - M_2, M_1 - M_2, \sin \alpha - v_2$ plane, where the region allowed by the theoretical constraints, and the LHC data at $\sqrt{s} = 13$ TeV are shown by blue and violet points respectively.

First, we consider the theoretical constraints that restrict the quartic couplings λ_i s of the scalar potential, which are shown by the blue points in the Fig. (1). It is clear from the plots that, we have a lower limit on the triplet VEV v_2 , which must be greater than 5 GeV. We also have an upper limit on m_5 as well as on m_H . The theoretical constraints ensure that, the mass of the members of the quintuplet and the mass of the heavier CP-even neutral scalar must be less than 600 GeV and 720 GeV respectively. With increasing m_H and m_5 , lesser region for v_2 is allowed. When the value of m_5 is approximately in between 80 – 200 GeV, almost all values of v_2 ranging approximately from 6 – 60 GeV are allowed. But after that, the allowed region for v_2 becomes more and more shortened as the minimum allowed value for v_2 is gradually shifted to the higher values. As v_2 increases, absolute value of M_1 also increases sharply, while that of M_2 decreases. There are also correlation between the trilinear coefficients M_1 and M_2 which can be seen from the plot. Also, there is no preferred value of $\sin \alpha$ with changing v_2 .

Next, we consider the LHC data at $\sqrt{s} = 13$ TeV, which are depicted by the violet points in the plots of the Fig. (1). No limit is offered on the masses and the trilinear coefficients M_1 and M_2 by the LHC data. But, we get a prominent allowed region in the $\sin \alpha - v_2$ plane from these data, which is mainly due to the inclusion of the charged scalars in the loop for the decay channel $h \rightarrow \gamma\gamma$. Mainly

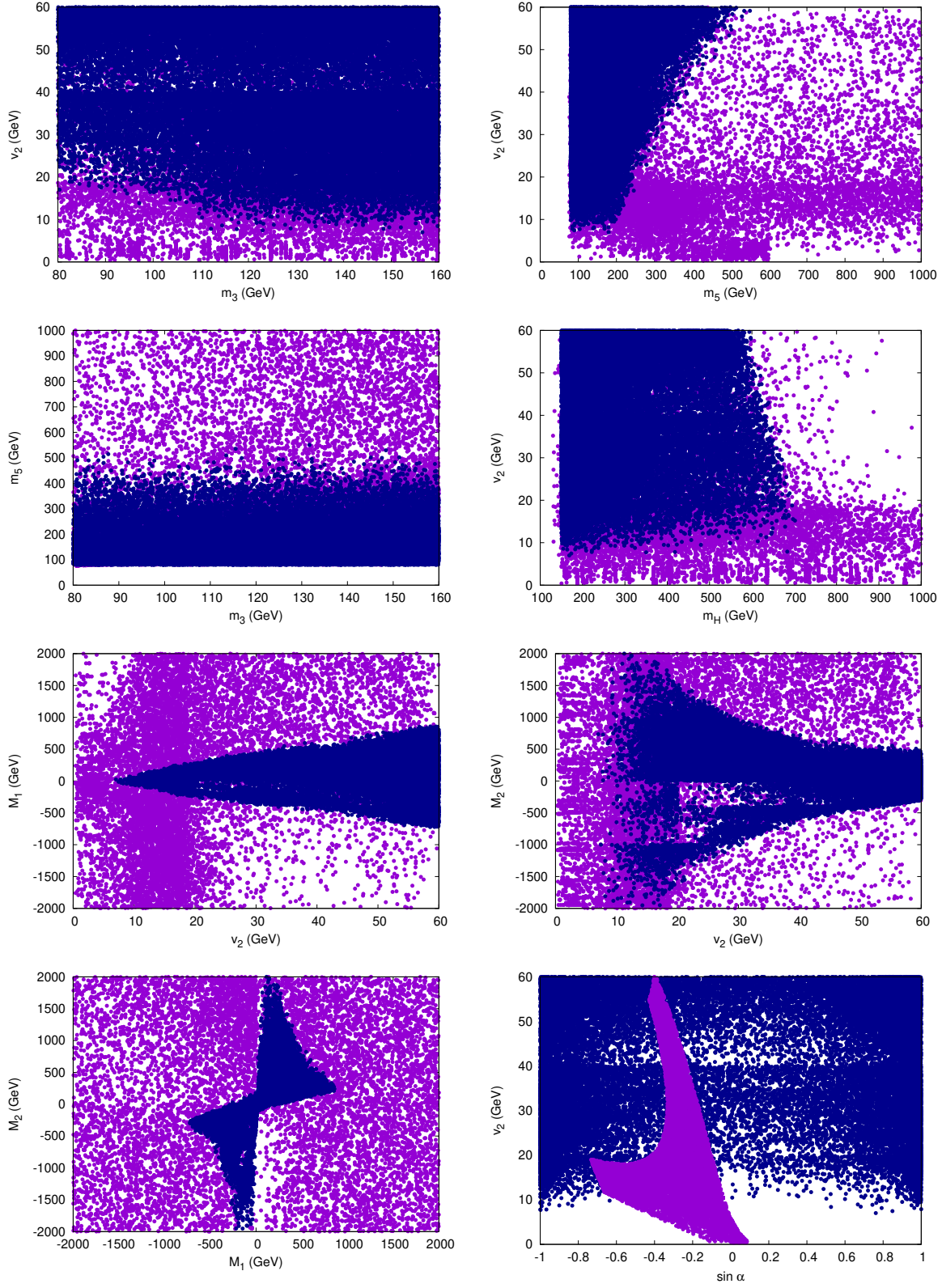


Figure 1: Allowed parameter space in the $m_3 - v_2$, $m_5 - v_2$, $m_3 - m_5$, $m_H - v_2$, $v_2 - M_1$, $v_2 - M_2$, $M_1 - M_2$, $\sin \alpha - v_2$ plane from theoretical constraints and LHC data at $\sqrt{s} = 13$ TeV, are shown by blue and violet points respectively.

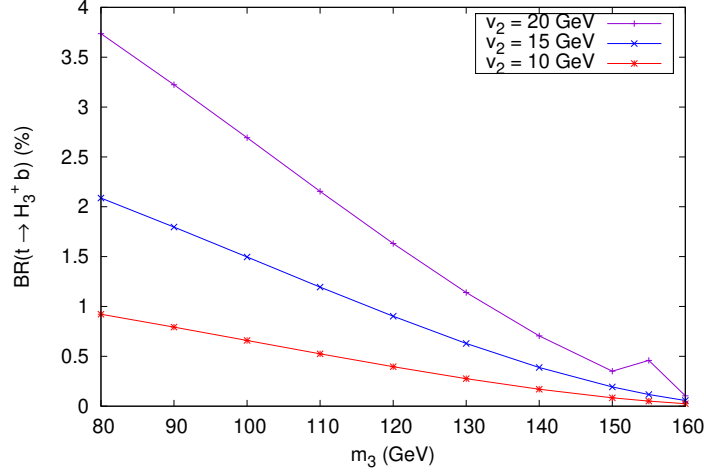


Figure 2: Branching ratio of $t \rightarrow H_3^+ b$ as a function of mass m_3 in GeV, for $v_2 = 10, 15, 20$ GeV. The other parameters chosen as mentioned in the Eq. (23).

negative values and some small positive values (< 0.15) of $\sin \alpha$ are admitted by the LHC data. For $v_2 > 10$ GeV, no positive values of $\sin \alpha$ is allowed and for $v_2 > 20$ GeV, a further narrow region is allowed in this plane.

It should be clear from the above discussion, that, the theoretical constraints or the LHC data alone cannot curb the parameter space, and hence we are to consider both of them simultaneously, which we show in the plots of the Fig. 1 by the points in the region overlapped by both of the blue and violet points. For instance, consider the $v_2 - m_H$ plane, where, though the LHC data do not put any limit on m_H , the theoretical constraints admit the value of m_H upto 700 GeV. The plots in the Fig. 1 clearly admit that, though the limits on the masses (m_H, m_3, m_5) and the trilinear couplings (M_1, M_2) are mainly arising due to the adoption of the theoretical constraints, the limits on the triplet VEV v_2 and $\sin \alpha$ are direct consequence of the application of the LHC data.

4 Results

We have already mentioned that, in the GM model, there are two pairs of singly charged scalars; H_3^\pm coming from the triplet and H_5^\pm coming from the quintuplet. But, due to its pure triplet origin, H_5^\pm do not couple to the SM fermions, while H_3^\pm couple to the fermions via the doublet mixing, which can also be observed from the Eq. (10). In this paper, we are interested only in fermionic decay of the singly charged scalars, and therefore, we will talk about the branching ratios of H_3^\pm . Since we focus only on the decays of the light charged scalar, in this paper, the production process of H_3^\pm we consider is through the decay of t (or \bar{t}) to $H_3^+ b$ ($H_3^- \bar{b}$).

First, in the Fig. 2 we depict the branching ratio (BR) of $t \rightarrow H_3^+ b$ for varying v_2 and show that, for a particular mass of H_3^+ , BR increases with increasing v_2 , while it decreases with increasing mass at any fixed triplet VEV. Here, we consider three values of v_2 ; 10, 15, 20 GeV. Though the BR of the decay $t \rightarrow W^+ b$ is maximum, that of $t \rightarrow H_3^+ b$ is still sizeable in the GM model. In the Fig. 3, we show the BR of H_3^\pm as the function of mass m_3 . We only depict the decays of H_3^\pm for which the corresponding BR is greater than 0.0001. To generate these plots (Fig. 2, 3), we choose,

$$m_H = 200 \text{ GeV}, m_5 = 80 \text{ GeV}, \sin \alpha = -0.2, M_1 = M_2 = 100 \text{ GeV}, \quad (23)$$

such that, the selection of the parameters satisfy the theoretical constraints given in the Sec. 3. To plot

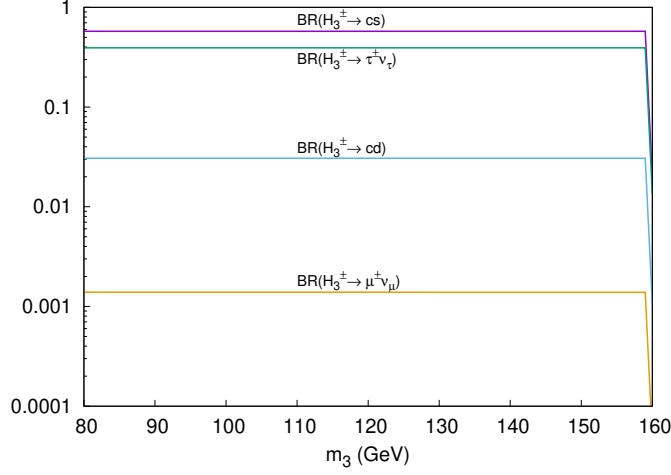


Figure 3: Branching ratios of H_3^\pm as a function of mass m_3 in GeV at $v_2 = 20$ GeV. The other independent parameters are chosen as mentioned in the Eq. (23).

the Fig. 3, we choose a particular value of the triplet VEV $v_2 = 20$ GeV, as the nature of this plot is independent of the value of v_2 .

The plots in this Fig. show that, the BR is maximum for the process $H_3^\pm \rightarrow cs$ followed by the process $H_3^\pm \rightarrow \tau^\pm \nu_\tau$ with an approximate value of 0.57 and 0.39 respectively. Therefore, we are interested in probing the parameter space of the GM model for the light (within the mass range 80 – 160 GeV) singly charged scalar H_3^\pm produced by the mechanism $t \rightarrow H_3^\pm b$, with the subsequent decays $H_3^\pm \rightarrow cs$ and $H_3^\pm \rightarrow \tau^\pm \nu_\tau$.

Light charged Higgs boson decaying via $H^\pm \rightarrow cs$ has already been searched in CMS with $\sqrt{s} = 13$ TeV [5]. Also, search for light charged Higgs boson in the $H^\pm \rightarrow \tau^\pm \nu_\tau$ decay is already carried out in ATLAS [8] and CMS [9] with $\sqrt{s} = 13$ TeV. We use these experimental results to provide an upper limit on the triplet VEV v_2 in the GM model.

We depict $BR(t \rightarrow H_3^\pm b) \times BR(H_3^\pm \rightarrow c\bar{s})$ as a function of the charged scalar mass (m_3) for three choices of triplet VEV v_2 in the Fig. 4. From the plot, one can see that, for $v_2 = 20$ GeV, a very narrow region of mass, $m_3 > 147$ GeV, is only allowed. The scenario becomes better with decreasing v_2 . For $v_2 = 15$ GeV, the charged scalar mass less than 85 GeV and greater than 137 GeV is allowed. For $v_2 = 10$ GeV, only the region with mass in between 95 – 118 GeV, approximately, is excluded. The full mass region is available for further decrease in v_2 , which is not shown in this plot, but can easily be understood.

Next, we depict the plots for the decay of H_3^\pm into $\tau^\pm \nu_\tau$ but in two different manners to apply the bound obtained from the data by ATLAS and CMS, separately. In the left plot of the Fig. 5, we show production cross section ($\sigma_{H_3^\pm}$) times branching ratio of H_3^\pm decaying into $\tau^\pm \nu_\tau$ as a function of mass m_3 in GeV, for $v_2 = 15, 20$ GeV. Following [9], we consider $\sigma_{H_3^\pm} = 2\sigma_{t\bar{t}} BR(t \rightarrow H_3^\pm b)(1 - BR(t \rightarrow H_3^\pm b))$. Here, the shaded region is excluded by CMS data. From the plot, one can see that, for $v_2 = 20$ GeV, the region with mass greater than 130 GeV is only allowed. For $v_2 = 15$ GeV, the full mass range is allowed. In the right plot of the Fig. 5, we show BR of the top quark decaying into $H_3^\pm b$ times BR of H_3^\pm decaying into $\tau^\pm \nu_\tau$ as a function of mass m_3 in GeV, for $v_2 = 10, 15, 20$ GeV. Here, the black line represents the limit from ATLAS experiment [8]. From the plot, one can see that, a very narrow region is allowed by the experimental data. The region with $m_3 > 146$ GeV, approximately, is allowed for this decay for $v_2 = 10$ GeV. For $v_2 = 15$ and 20 GeV, this allowed mass region is above 157 and 158 GeV respectively. Therefore, for this decay channel, ATLAS provides a more stringent bound on the triplet VEV than CMS.

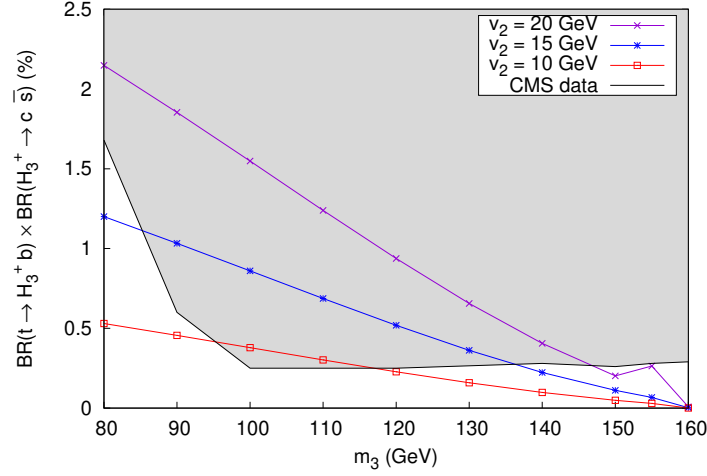


Figure 4: Branching ratio of the top quark decaying into H_3^+ and b times the branching ratio of H_3^+ decaying into c and \bar{s} as a function of mass m_3 in GeV, for $v_2 = 10, 15, 20$ GeV with red, blue and violet coloured lines respectively. The black line represents the limit from CMS experiment [5]. The shaded region is excluded by CMS data.

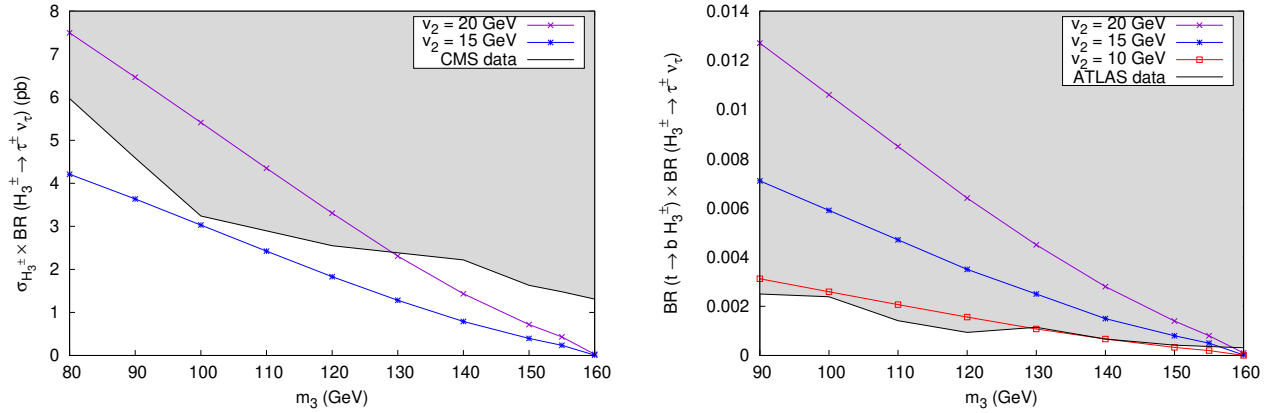


Figure 5: Left : Production cross section times branching ratio of H_3^\pm decaying into $\tau^\pm \nu_\tau$ as a function of mass m_3 in GeV, for $v_2 = 15, 20$ GeV. The black line represents the limit from CMS experiment [9]. Right : Branching ratio of the top quark decaying into H_3^\pm and b times the branching ratio of H_3^\pm decaying into $\tau^\pm \nu_\tau$ as a function of mass m_3 in GeV, for $v_2 = 10, 15, 20$ GeV. The black line represents the limit from ATLAS experiment [8].

The red, blue and violet lines correspond to $v_2 = 10, 15, 20$ GeV respectively. The shaded region is excluded by the experimental data.

To generate the plots, we first implement the model in Feynrules [46] to obtain the UFO file required to generate events using MadGraph5 (v2.8.2) [47].

5 Conclusions

Recent searches at the LHC for light singly-charged scalar decaying into either cs or $\tau^\pm\nu_\tau$ encourage us to investigate these decay channels in BSM model with triplets. We choose the Georgi-Machacek model, where the scalar sector of SM is added by a real and a complex triplet, such that, the custodial symmetry is preserved at the tree level. Besides two doubly charged scalars, there are four singly-charged scalars in this model, out of which two (H_5^\pm) do not have any couplings with the SM fermions. Therefore, we are interested in the production and decay of the other two singly-charged scalars (H_3^\pm). Since, we consider only the decay of light charged scalars, within the mass range of 80 – 160 GeV, the production mechanism we contemplate is $t \rightarrow H_3^\pm b$. We get an upper bound on the triplet VEV by considering the experimental limits provided by ATLAS and CMS at the LHC with $\sqrt{s} = 13$ TeV, for the decay channels $H_3^\pm \rightarrow cs$ and $H_3^\pm \rightarrow \tau^\pm\nu_\tau$, separately. For $H_3^\pm \rightarrow cs$, the full mass range of m_3 is not available even for $v_2 = 10$ GeV, and we must lower the triplet VEV further to employ the full range of m_3 (i.e., 80 – 160 GeV), while in the case of $H_3^\pm \rightarrow \tau^\pm\nu_\tau$, lowering v_2 below 10 GeV may give the full access of the lower range of m_3 . It is also to be noted that, for the former case, data from the CMS experiment are only available, whereas, for the later, though the data are available from ATLAS and CMS both, we get a more stringent bound from the ATLAS. On top of this, we also considered the restrictions on the parameter space arising from the theoretical constraints and Higgs data. We showed that, simultaneous adoption of these constraints also curb the parameter space of the GM model.

Acknowledgements — The author would like to acknowledge the SERB grant CRG/2018/004889. SG also thanks Prof. Anirban Kundu for useful discussions and Dr. Suman Chatterjee for technical help in MadGraph5. This work is done independently, without any financial support, as the author is an honorary fellow.

References

- [1] G. Aad *et al.* [ATLAS], Phys. Lett. B **716**, 1-29 (2012) doi:10.1016/j.physletb.2012.08.020 [arXiv:1207.7214 [hep-ex]].
- [2] S. Chatrchyan *et al.* [CMS], Phys. Lett. B **716**, 30-61 (2012) doi:10.1016/j.physletb.2012.08.021 [arXiv:1207.7235 [hep-ex]].
- [3] A. Ivina [ATLAS], PoS **EPS-HEP2021**, 631 (2022) doi:10.22323/1.398.0631
- [4] [ATLAS], ATLAS-CONF-2021-037.
- [5] A. M. Sirunyan *et al.* [CMS], Phys. Rev. D **102**, no.7, 072001 (2020) doi:10.1103/PhysRevD.102.072001 [arXiv:2005.08900 [hep-ex]].
- [6] G. Aad *et al.* [ATLAS], Eur. Phys. J. C **73**, no.6, 2465 (2013) doi:10.1140/epjc/s10052-013-2465-z [arXiv:1302.3694 [hep-ex]].
- [7] [ATLAS], ATL-PHYS-PUB-2010-006.
- [8] M. Aaboud *et al.* [ATLAS], JHEP **09**, 139 (2018) doi:10.1007/JHEP09(2018)139 [arXiv:1807.07915 [hep-ex]].
- [9] A. M. Sirunyan *et al.* [CMS], JHEP **07**, 142 (2019) doi:10.1007/JHEP07(2019)142 [arXiv:1903.04560 [hep-ex]].

- [10] S. Abbaspour, S. M. Moosavi Nejad and M. Balali, Nucl. Phys. B **932**, 505-528 (2018) doi:10.1016/j.nuclphysb.2018.05.023 [arXiv:1806.02546 [hep-ph]].
- [11] M. Aaboud *et al.* [ATLAS], Phys. Lett. B **759**, 555-574 (2016) doi:10.1016/j.physletb.2016.06.017 [arXiv:1603.09203 [hep-ex]].
- [12] [ATLAS], ATLAS-CONF-2011-151.
- [13] G. Aad *et al.* [ATLAS], JHEP **06**, 039 (2012) doi:10.1007/JHEP06(2012)039 [arXiv:1204.2760 [hep-ex]].
- [14] A. Ali, F. Barreiro and J. Llorente, Eur. Phys. J. C **71**, 1737 (2011) doi:10.1140/epjc/s10052-011-1737-8 [arXiv:1103.1827 [hep-ph]].
- [15] S. Chatrchyan *et al.* [CMS], JHEP **07**, 143 (2012) doi:10.1007/JHEP07(2012)143 [arXiv:1205.5736 [hep-ex]].
- [16] K. Cheung, A. Jueid, J. Kim, S. Lee, C. T. Lu and J. Song, [arXiv:2201.06890 [hep-ph]].
- [17] A. G. Akeroyd, M. Aoki, A. Arhrib, L. Basso, I. F. Ginzburg, R. Guedes, J. Hernandez-Sanchez, K. Huitu, T. Hurth and M. Kadastik, *et al.* Eur. Phys. J. C **77**, no.5, 276 (2017) doi:10.1140/epjc/s10052-017-4829-2 [arXiv:1607.01320 [hep-ph]].
- [18] R. Benbrik, M. Boukidi, B. Manaut, M. Ouchemhou, S. Semlali and S. Taj, [arXiv:2112.07502 [hep-ph]].
- [19] A. G. Akeroyd, S. Moretti, K. Yagyu and E. Yildirim, Int. J. Mod. Phys. A **32**, no.23n24, 1750145 (2017) doi:10.1142/S0217751X17501457 [arXiv:1605.05881 [hep-ph]].
- [20] A. G. Akeroyd, S. Moretti and J. Hernandez-Sanchez, Phys. Rev. D **85**, 115002 (2012) doi:10.1103/PhysRevD.85.115002 [arXiv:1203.5769 [hep-ph]].
- [21] A. G. Akeroyd, S. Moretti and M. Song, [arXiv:2202.03522 [hep-ph]].
- [22] W. S. Hou, R. Jain and T. Modak, [arXiv:2111.06523 [hep-ph]].
- [23] A. G. Akeroyd, S. Moretti and M. Song, Phys. Rev. D **101**, no.3, 035021 (2020) doi:10.1103/PhysRevD.101.035021 [arXiv:1908.00826 [hep-ph]].
- [24] A. G. Akeroyd, S. Moretti and M. Song, Phys. Rev. D **98**, no.11, 115024 (2018) doi:10.1103/PhysRevD.98.115024 [arXiv:1810.05403 [hep-ph]].
- [25] H. Georgi and M. Machacek, Nucl. Phys. B **262**, 463-477 (1985) doi:10.1016/0550-3213(85)90325-6
- [26] N. Ghosh, S. Ghosh and I. Saha, Phys. Rev. D **101**, no.1, 015029 (2020) doi:10.1103/PhysRevD.101.015029 [arXiv:1908.00396 [hep-ph]].
- [27] H. E. Logan and Y. Wu, JHEP **11**, 121 (2018) doi:10.1007/JHEP11(2018)121 [arXiv:1809.09127 [hep-ph]].
- [28] A. Ismail, H. E. Logan and Y. Wu, [arXiv:2003.02272 [hep-ph]].
- [29] K. Hartling, K. Kumar and H. E. Logan, Phys. Rev. D **90**, no.1, 015007 (2014) doi:10.1103/PhysRevD.90.015007 [arXiv:1404.2640 [hep-ph]].
- [30] M. E. Krauss and F. Staub, Eur. Phys. J. C **78**, no.3, 185 (2018) doi:10.1140/epjc/s10052-018-5676-5 [arXiv:1709.03501 [hep-ph]].

- [31] G. Moultağa and M. C. Peyranère, Phys. Rev. D **103**, no.11, 115006 (2021) doi:10.1103/PhysRevD.103.115006 [arXiv:2012.13947 [hep-ph]].
- [32] M. Aoki and S. Kanemura, Phys. Rev. D **77**, no.9, 095009 (2008) [erratum: Phys. Rev. D **89**, no.5, 059902 (2014)] doi:10.1103/PhysRevD.77.095009 [arXiv:0712.4053 [hep-ph]].
- [33] K. Hartling, K. Kumar and H. E. Logan, Phys. Rev. D **91**, no.1, 015013 (2015) doi:10.1103/PhysRevD.91.015013 [arXiv:1410.5538 [hep-ph]].
- [34] J. Chang, C. R. Chen and C. W. Chiang, JHEP **03**, 137 (2017) doi:10.1007/JHEP03(2017)137 [arXiv:1701.06291 [hep-ph]].
- [35] C. W. Chiang and T. Yamada, Phys. Lett. B **735**, 295-300 (2014) doi:10.1016/j.physletb.2014.06.048 [arXiv:1404.5182 [hep-ph]].
- [36] R. Zhou, W. Cheng, X. Deng, L. Bian and Y. Wu, JHEP **01**, 216 (2019) doi:10.1007/JHEP01(2019)216 [arXiv:1812.06217 [hep-ph]].
- [37] A. Banerjee, G. Bhattacharyya and N. Kumar, Phys. Rev. D **99**, no.3, 035028 (2019) doi:10.1103/PhysRevD.99.035028 [arXiv:1901.01725 [hep-ph]].
- [38] C. W. Chiang, S. Kanemura and K. Yagyu, Phys. Rev. D **90**, no.11, 115025 (2014) doi:10.1103/PhysRevD.90.115025 [arXiv:1407.5053 [hep-ph]].
- [39] C. W. Chiang, S. Kanemura and K. Yagyu, Phys. Rev. D **93**, no.5, 055002 (2016) doi:10.1103/PhysRevD.93.055002 [arXiv:1510.06297 [hep-ph]].
- [40] H. E. Logan and V. Rentala, Phys. Rev. D **92**, no.7, 075011 (2015) doi:10.1103/PhysRevD.92.075011 [arXiv:1502.01275 [hep-ph]].
- [41] A. Kundu, P. Mondal and P. B. Pal, [arXiv:2111.14195 [hep-ph]].
- [42] K. Hartling, K. Kumar and H. E. Logan, [arXiv:1412.7387 [hep-ph]].
- [43] C. W. Chiang, G. Cottin and O. Eberhardt, Phys. Rev. D **99**, no.1, 015001 (2019) doi:10.1103/PhysRevD.99.015001 [arXiv:1807.10660 [hep-ph]].
- [44] [CMS], CMS-PAS-HIG-17-031.
- [45] [ATLAS], ATLAS-CONF-2019-005.
- [46] A. Alloul, N. D. Christensen, C. Degrande, C. Duhr and B. Fuks, Comput. Phys. Commun. **185**, 2250-2300 (2014) doi:10.1016/j.cpc.2014.04.012 [arXiv:1310.1921 [hep-ph]].
- [47] J. Alwall, R. Frederix, S. Frixione, V. Hirschi, F. Maltoni, O. Mattelaer, H. S. Shao, T. Stelzer, P. Torrielli and M. Zaro, JHEP **07**, 079 (2014) doi:10.1007/JHEP07(2014)079 [arXiv:1405.0301 [hep-ph]].